



UNIVERSITÀ
DEGLI STUDI
FIRENZE

FLORE

Repository istituzionale dell'Università degli Studi di Firenze

Mesoscopic optical imaging of whole mouse heart

Questa è la Versione finale referata (Post print/Accepted manuscript) della seguente pubblicazione:

Original Citation:

Mesoscopic optical imaging of whole mouse heart / Giardini F.; Lazzeri E.; Olianti C.; Beconi G.; Costantini I.; Silvestri L.; Cerbai E.; Pavone F.S.; Sacconi L.. - In: JOURNAL OF VISUALIZED EXPERIMENTS. - ISSN 1940-087X. - ELETTRONICO. - 2021:(2021), pp. 0-0. [10.3791/62795]

Availability:

The webpage <https://hdl.handle.net/2158/1260658> of the repository was last updated on 2022-05-06T16:26:20Z

Published version:

DOI: 10.3791/62795

Terms of use:

Open Access

La pubblicazione è resa disponibile sotto le norme e i termini della licenza di deposito, secondo quanto stabilito dalla Policy per l'accesso aperto dell'Università degli Studi di Firenze (<https://www.sba.unifi.it/upload/policy-oa-2016-1.pdf>)

Publisher copyright claim:

Conformità alle politiche dell'editore / Compliance to publisher's policies

Questa versione della pubblicazione è conforme a quanto richiesto dalle politiche dell'editore in materia di copyright.

This version of the publication conforms to the publisher's copyright policies.

La data sopra indicata si riferisce all'ultimo aggiornamento della scheda del Repository FloRe - The above-mentioned date refers to the last update of the record in the Institutional Repository FloRe

(Article begins on next page)

Authors' version –

Published source Giardini, F., Lazzeri, E., Olianti, C., Beconi, G., Costantini, I., Silvestri, L., Cerbai, E., Pavone, F. S., Sacconi, L. Mesoscopic Optical Imaging of Whole Mouse Heart. *J. Vis. Exp.* (176), e62795, doi:10.3791/62795 (2021).

LINK to Published version <https://www.jove.com/it/t/62795/mesoscopic-optical-imaging-of-whole-mouse-heart>

Copyright: Journal of Visualized Experiments

TITLE:

Mesoscopic Optical Imaging of Whole Mouse Heart

AUTHORS AND AFFILIATIONS:

Francesco Giardini^{1,*}, Erica Lazzeri^{1,*}, Camilla Olianti^{1,*}, Giada Beconi¹, Irene Costantini^{1,2}, Ludovico Silvestri^{1,3,4}, Elisabetta Cerbai^{1,5}, Francesco S. Pavone^{1,3,4}, Leonardo Sacconi^{1,3,#}

¹European Laboratory for Non-Linear Spectroscopy, Sesto Fiorentino, 50019, Italy.

²Department of Biology, University of Florence, Sesto Fiorentino, 50019, Italy.

³National Institute of Optics, National Research Council, Florence, 50125, Italy.

⁴Department of Physics and Astronomy, University of Florence, Sesto Fiorentino, 50019, Italy.

⁵Department of Neurosciences, Psychology, Drugs and Child Health, University of Florence, Italy.

* The authors contributed equally to the work.

Email addresses of co-authors:

Francesco Giardini	(giardini@lens.unifi.it)
Erica Lazzeri	(lazzierica@gmail.com)
Camilla Olianti	(olianti@lens.unifi.it)
Giada Beconi	(giada.beconi@gmail.com)
Irene Costantini	(costantini@lens.unifi.it)
Ludovico Silvestri	(silvestri@lens.unifi.it)
Elisabetta Cerbai	(cerbai@lens.unifi.it)
Francesco S. Pavone	(pavone@lens.unifi.it)
Leonardo Sacconi	(sacconi@lens.unifi.it)

#Corresponding author:

Leonardo Sacconi (sacconi@lens.unifi.it)

SUMMARY:

We report a method for mesoscopic reconstruction of the whole mouse heart by combining new advancements in tissue transformation and staining with the development of an axially scanned light-sheet microscope.

ABSTRACT:

Both genetic and non-genetic cardiac diseases can cause severe remodeling processes in the heart. Structural remodeling, such as collagen deposition (fibrosis) and cellular misalignment, can affect electrical conduction, introduce electromechanical dysfunctions and, eventually lead to arrhythmia. Current predictive models of these functional alterations are based on non-integrated and low-resolution structural information. Placing this framework on a different order of magnitude is

challenging due to the inefficacy of standard imaging methods in performing high-resolution imaging in massive tissue. In this work, a new methodological framework is described that allows imaging of whole mouse hearts with micrometric resolution. The achievement of this goal has required an impressive technological effort where advances in tissue transformation and imaging methods have been combined. First, we describe an optimized CLARITY protocol capable of transforming an intact heart into a nanoporous, hydrogel-hybridized, lipid-free form that allows high transparency and deep staining is described. Then, a fluorescence light-sheet microscope able to rapidly acquire images of a mesoscopic field of view (mm-scale) with the micron-scale resolution is described. Inspired by the mesoSPIM project, the conceived microscope allows the reconstruction of the whole mouse heart with micrometric resolution in a single tomographic scan. We believe that this methodological framework will allow clarifying the involvement of the cytoarchitecture disarray in the electrical dysfunctions and pave the way for a comprehensive model that considers both the functional and structural data, thus enabling a unified investigation of the structural causes that lead to the electrical and mechanical alterations after the tissue remodeling.

INTRODUCTION:

Structural remodeling associated with cardiac diseases can affect electrical conduction and introduce electromechanical dysfunctions of the organ^{1,2}. Current approaches used to predict functional alterations commonly employ MRI and DT-MRI to obtain an overall reconstruction of fibrosis deposition, vascular tree, and fiber distribution of the heart, and they are used to model preferential action potential propagation (APP) paths across the organ^{3,4}. These strategies can provide a beautiful overview of the heart organization. However, their spatial resolution is insufficient to investigate the impact of structural remodeling on cardiac function at the cellular level.

Placing this framework at a different order of magnitude, where single cells can play individual roles on action potential propagation, is challenging. The main limitation is the inefficiency of standard imaging methods to perform high-resolution imaging (micrometric resolution) in massive (centimeter-sized) tissues. In fact, imaging biological tissues in 3D at high resolution is very complicated due to tissue opaqueness. The most common approach to perform 3D reconstructions in entire organs is to prepare thin sections. However, precise sectioning, assembling, and imaging require significant effort and time. An alternative approach that does not demand cutting the sample is to generate a transparent tissue. During the last years, several methodologies for clarifying tissues have been proposed⁵⁻⁸. The challenge to produce massive, transparent, and fluorescently-labeled tissues has been recently achieved by developing true tissue transformation approaches (CLARITY⁹, SHIELD¹⁰). In particular, the CLARITY method is based on the transformation of an intact tissue into a nanoporous, hydrogel-hybridized, lipid-free form that enables to confer high transparency by the selective removal of membrane lipid bilayers. Notably, this method has been found successful also in cardiac preparation¹¹⁻¹⁴. However, since the heart is too fragile to be suitable for an active clearing, it must be cleared using the passive approach, which requires a long time to confer complete transparency.

In combination with advanced imaging techniques like light-sheet microscopy, CLARITY has the potential to image 3D massive heart tissues at micrometric resolution. In light-sheet microscopy, the illumination of the sample is performed with a thin sheet of light confined in the focal plane of the detection objective. The fluorescence emission is collected along an axis perpendicular to the illumination plane¹⁵. The detection architecture is similar to widefield microscopy, making the acquisition much faster than laser scanning microscopes. Moving the sample through the light sheet permits obtaining a complete tomography of big specimens, up to centimeter-sized samples.

However, due to the intrinsic properties of the Gaussian beam, it is possible to obtain a very thin (of the order of a few microns) light-sheet only for a limited spatial extension, thus drastically limiting the field of view (FoV). Recently, a novel excitation scheme has been introduced to overcome this limitation and applied for brain imaging, allowing 3d reconstructions with isotropic resolution¹⁶.

In this paper, a passive clearing approach is presented, enabling a significant reduction of the clearing timing needed by the CLARITY protocol. The methodological framework described here allows reconstructing a whole mouse heart with micrometric resolution in a single tomographic scan with an acquisition time in the order of minutes.

PROTOCOL:

All animal handling and procedures were performed in accordance with the guidelines from Directive 2010/63/EU of the European Parliament on the protection of animals used for scientific purposes and conformed to the principles and regulations of the Italian Ministry of Health. The experimental protocol was approved by the Italian Ministry of Health (protocol number 647/2015-PR). All the animals were provided by ENVIGO, Italy. For these experiments, 5 male C57BL/6J mice of 6 months of age were used.

1. Solution preparation

1.1. Prepare 4% Paraformaldehyde (PFA) in Phosphate-Buffered Saline (PBS) (pH 7.6) in a chemical hood. Store the 4% PFA aliquots at -20 °C for several months.

1.2. Prepare Hydrogel solution: Mix 4% Acrylamide, 0.05% Bis-acrylamide, 0.25% Initiator AV-044 in 0.01 M PBS in a chemical hood. Keep the reagents and the solution on ice during the entire preparation. Store the hydrogel aliquots at -20 °C for several months.

1.3. Prepare Clearing solution: Mix 200 mM Boric acid, 4% Sodium Dodecyl-Sulfate (SDS) in deionized water; pH 8.6 in a chemical hood. Store the solution between 21–37 °C to avoid SDS precipitation.

1.4. Prepare fresh Tyrode solution on the day of the experiment: Add 10 mM Glucose, 10 mM HEPES, 113 mM NaCl, 1.2 mM MgCl₂, and 4.7 mM KCl; titrate to pH 7.4 using 1 M NaOH.

2. Heart isolation

2.1. Inject 0.1 mL of 500 I.U. Heparin subcutaneously 30 min before the heart isolation procedure.

2.2. Fill a 30-mL syringe and three 6-cm Petri dishes with fresh Tyrode solution. Make a small rift (3–4 mm in depth) on the border of one of the Petri dishes and place it under a stereoscopic microscope.

2.3. Fix a 1 mm-diameter cannula to the syringe and insert it in the rift of the Petri dish. Make sure there are no air bubbles in the syringe.

2.4. Fill a 20-mL syringe with 4% PFA and keep it in the chemical hood. Prepare an empty Petri dish under the hood.

2.5. Anesthetize the mouse with 3% Isoflurane/oxygen at a flow rate of 1.0 L/min and sacrifice it by cervical dislocation according to animal welfare rules in force.

148
149 2.6. After the sacrifice, remove the fur over the chest and open the chest to have full access to the
150 heart.
151
152 2.7. Isolate the heart, immerse it in the Petri dish previously filled with 50 mL of Tyrode Solution.
153 Use surgical scissors to cut the aorta immediately near the aortic arch to have the heart exposed.
154
155 2.8. Transfer the heart under a stereoscopic microscope and carefully perform the cannulation. Do
156 not insert the cannula too deep into the aorta (no more than 2 mm) to avoid tissue damage.
157
158 2.9. Use a little clamp and a suture (size 5/0) to fix the heart to the cannula.
159
160 2.10. Perfuse the heart with 30 mL of the Tyrode solution with a constant pressure of 10 mL/min to
161 remove blood from the vessels.
162
163 2.11. Detach the cannula from the syringe and place the heart in the Petri dish filled with Tyrode
164 solution. Be careful not to have air bubbles in the cannula; otherwise, remove the air bubbles
165 properly.
166
167 2.12. Attach the 20-mL syringe filled with cold 4% PFA to the cannula and perfuse the heart at the
168 same constant pressure.
169
170 2.13. Incubate the heart in 10 mL of 4% PFA at 4 °C overnight (O/N). To avoid tissue degradation,
171 perform steps 2.6–2.13 in the shortest time possible.
172
173 **3. Heart clearing**
174
175 3.1. The following day, wash the heart in 0.01 M PBS 3 times at 4 °C for 15 min.
176
177 NOTE: After this step, the heart can be stored in PBS + 0.01% sodium azide (NaN₃) at 4 °C for several
178 months.
179
180 3.2. Incubate the heart in 30 mL of Hydrogel solution in shaking (15 rpm) at 4 °C for 3 days.
181
182 3.3. Degas the sample at room temperature using a dryer, a vacuum pump, and a tube system that
183 connects the dryer to both the pump and a nitrogen pipeline.
184
185 3.3.1. Place the sample in the dryer and open the vial, keeping the cap on it.
186
187 3.3.2. Close the dryer and remove the oxygen from the tube by opening the nitrogen pipeline.
188
189 3.3.3. Turn on the vacuum pump to remove the oxygen from the dryer for 10 min.
190
191 3.3.4. Turn off the pump and use the knob of the dryer to open the nitrogen pipeline. Once the
192 pressure is equal to the atmospheric pressure, carefully open the dryer and quickly close the vial.
193
194 3.4. Keep the heart in the degassed Hydrogel solution at 37 °C for 3 h at rest.
195

196 3.5. When the Hydrogel is properly polymerized and appears entirely gelatinous, carefully remove
197 the heart from it and place it in the sample holder.

198
199 3.6. Insert the sample holder with the heart in one of the clearing chambers and close it properly to
200 avoid leaks of the clearing solution.

201
202 3.7. Switch on the water bath where the clearing solution container is placed and the peristaltic
203 pump to start the recirculation of the clearing solution.

204
205 3.8. Change the clearing solution in the container once a week to speed up the clarification
206 procedure.

207
208 **4. Cellular membrane staining**

209
210 4.1. Once the heart appears completely clarified, remove it from the sample holder and wash it in
211 50 mL of warmed-up PBS for 24 h. Wash again in 50 mL of PBS + 1% of Triton-X (PBS-T 1x) for 24 h.

212
213 4.2. Incubate the sample in 0.01 mg/mL Wheat Germ Agglutinin (WGA) – Alexa Fluor 633 in 3 mL of
214 PBS-T 1x in shaking (50 rpm) at room temperature for 7 days.

215
216 4.3. After the 7-day incubation, wash the sample in 50 mL of PBS-T 1x at room temperature in
217 shaking for 24 h.

218
219 4.4. Incubate the sample in 4% PFA for 15 min and then wash it 3 times in PBS for 5 min each.

220
221 NOTE: After this step, the heart can be stored in PBS + 0.01% NaN₃ at 4 °C for several months.

222
223 4.5. Incubate the heart in increasing concentrations of 2,2'-Thiodiethanol (TDE) in 0.01 M PBS (20%
224 and 47% TDE/PBS) for 8 h each, up to the final concentration of 68% TDE in 0.01 M PBS to provide
225 the required refractive index (RI = 1.46). This is the RI matching medium (RI-medium) to acquire
226 images¹⁶.

227
228 **5. Heart mounting and acquisition**

229
230 NOTE: All the components of the optical system are listed in detail in the **Table of Materials**.

231
232 5.1. Gently fill about 80% of the external cuvette (quartz, 45 mm × 45 mm × 42.5 mm) with the RI-
233 medium.

234
235 NOTE: Here, it is possible to use different non-volatile solutions that guarantee a RI of 1.46.

236
237 5.2. Gently fill the internal cuvette (quartz, 45 mm × 12.5 mm × 12.5 mm) with the same RI-medium.

238
239 5.3. Immerse the sample inside the internal cuvette. The sample incubations described above allow
240 the sample to remain stable inside the RI-medium without being held.

241
242 5.4. Gently move the sample to the bottom of the cuvette using thin tweezers and arrange the heart
243 with its longitudinal axis parallel to the cuvette's main axis to minimize the excitation light path
244 across the tissue during the scanning.

245
246 5.5. Gently fix the tailored plug above the internal cuvette with two screws.
247
248 5.6. Mount the sample to the microscope stage using the magnets.
249
250 5.7. Translate the vertical sample stage manually to immerse the internal cuvette into the external
251 one.
252
253 5.8. Turn on the excitation light source (wavelength of 638 nm), setting a low power (in the order of
254 3 mW).
255
256 5.9. Move the sample using the motorized translator to illuminate an inner plane of the tissue.
257
258 5.10. Turn on the imaging software (HCImageLive) and set the camera **Trigger** on **External Edge**
259 **Trigger (light-sheet)** mode to drive the acquisition trigger of the camera by the custom software
260 controlling the entire setup.
261
262 5.11. Enable **Autosave** in the **Scan Settings** panel and set the output folder where the images need
263 to be saved.
264
265 5.12. Manually adjust the sample position in the XY plane with the linear translators to move the
266 sample to the center of the FoV of the camera sensor.
267
268 5.13. Move the sample along the Z-axis using the linear motorized translator to identify heart
269 borders for tomographic reconstruction.
270
271 5.14. Increase the laser power to ~20 mW, ready for the imaging session.
272
273 5.15. Start the tomographic acquisition, click the **Start** button in the **Capture** panel of the imaging
274 software, and at the same time move the sample along the Z-axis at the constant velocity of 6 $\mu\text{m/s}$
275 using the motorized translator.
276

277 **REPRESENTATIVE RESULTS:**

278 The developed passive clearing setup allows to obtain a cleared adult mouse heart (with a dimension
279 of the order 10 mm x 6 mm x 6 mm) in about 3 months. All the components of the setup are
280 mounted, as shown in **Figure 1**. The negligible temperature gradient between each clearing chamber
281 (of the order of 3°C) allows maintaining the temperature in a proper range across all chambers.
282

283 [insert **Figure 1** here]
284

285 **Figure 2** shows the result of the clearing process of an entire heart. As already reported by Costantini
286 et al.¹⁶, the combination of the CLARITY methodology with TDE as RI-medium does not significantly
287 change the sample's final volume nor leads to anisotropic deformation of the specimen.
288

289 [insert **Figure 2** here]
290

291 Once the heart was cleared, cellular membranes were stained with an Alexa Fluor 633-conjugated
292 WGA to perform the cytoarchitecture reconstruction of the entire organ. The custom-made

fluorescence light-sheet microscope (**Figure 3**) was able to ensure 3D micron-scale resolution across the entire FoV.

[insert **Figure 3** here]

Considering the numerical aperture ($NA = 0.1$) of the detection optics, the radial (XY) Point Spread Function (PSF) of the system can be estimated in the order of $4\text{--}5\text{ }\mu\text{m}$. On the other hand, the excitation optics produce a light-sheet with a minimum waist of about $6\text{ }\mu\text{m}$ (Full width half maximum, FWHM) that diverges up to $175\text{ }\mu\text{m}$ at the edge of the FoV (**Figure 4A–C**). The synchronization of the camera rolling shutter with the axial scan of the light-sheet waist ensures to excite the sample with the thinnest portion of the light-sheet, resulting in an average FWHM of about $6.7\text{ }\mu\text{m}$ along the entire FoV (**Figure 4B–D**).

[insert **Figure 4** here]

The Z-PSF of the microscope was also estimated by a tomographic reconstruction of the fluorescent nanosphere (**Figure 5**). An FWHM of $6.4\text{ }\mu\text{m}$ can be estimated by the fit, in good agreement with the previous assessment.

[insert **Figure 5** here]

Owing to the high transparency of the tissue, it was possible to illuminate the whole heart without significant distortion of the axially scanned light-sheet at an excitation wavelength of 638 nm . The fluorescence signal was collected by the sCMOS sensor operating at 500 ms of exposure time and a frame rate of 1.92 Hz . Based on previous quantification, the tomographic acquisition was performed using a Z-scan velocity of $6\text{ }\mu\text{m/s}$, and assuming a frame rate of 1.92 Hz , one frame every $3.12\text{ }\mu\text{m}$ was acquired, oversampling the system Z-PSF by about two times. Two representative frames (on the coronal and transverse planes) of the left ventricle chamber are shown in **Figure 6**. This result confirms the potentiality of the system to resolve single cellular membranes in three dimensions with a sufficient Signal/Noise ratio in the entire organ (**Figure 6**).

[insert **Figure 6** here]

FIGURE AND TABLE LEGENDS:

Figure 1: Schematic of the passive clearing setup. The clearing solution (after being filtered) circulates in succession through the sample chambers with the help of the peristaltic pump. The maintenance of the solution container in a water bath set at $50\text{ }^{\circ}\text{C}$ allows the solution temperature to be between $37\text{--}45\text{ }^{\circ}\text{C}$ within the chambers. Image created with Biorender.com.

Figure 2: Representative image of a heart before (on the left) and after (on the right) the CLARITY protocol. The hearts become fully transparent and slightly oversized.

Figure 3: MesoSPIM. CAD renderings of the custom-made fluorescence light-sheet microscope.

Figure 4: Light-sheet generation and characterization. (A) An excitation light-sheet generated with a laser source of 638 nm is focused on the center of the Field of View (FoV) and acquired with a pixel size of $3.25\text{ }\mu\text{m}$ and an Exposure Time of 10 ms . Light intensity is normalized and reported with a colormap. The Full Width Half Maximum (FWHM) of the light intensity profile is evaluated in 15 different positions along the FoV. Results are shown in C. (B) Image of the excitation light-sheet

generated by the synchronization between the camera rolling shutter operating at 1.92 Hz and the light beam position driven by the tunable lens. The FWHM of the light intensity profile is evaluated along the FoV and results are shown in **D**.

Figure 5: Point Spread Function in the Z-axis. The Point Spread Function (PSF) of the optical system is estimated by imaging fluorescent sub-micron-scale nanospheres (excited with a light sheet with a wavelength of 638 nm) with a pixel size of $3.25\ \mu\text{m} \times 3.25\ \mu\text{m} \times 2.0\ \mu\text{m}$. PSF intensity profile along the optical axis (Z) is represented as black dots. PSF profile is fitted with a Gaussian function with $\mu = 18.6\ \mu\text{m}$ and $\sigma = 2.7\ \mu\text{m}$. The FWHM of the PSF estimated by the fit is $6.4\ \mu\text{m}$.

Figure 6: Mouse heart tissue reconstruction. The clarified heart was stained with WGA conjugated to Alexa Fluor 633 and excited by a laser source with a wavelength of 638 nm. **(A)** Coronal and **(B)** transverse representative sections. **(C–D)** Tissue transformation produces high tissue transparency, allowing to resolve small structures in the wall depth. The optical system shows an axial resolution sufficient to resolve micrometric structures (panel. **D**). **(E)** 3D low-resolution heart rendering.

DISCUSSION:

In this work, a successful approach to clear, stain, and image a whole mouse heart at high resolution was introduced. First, a tissue transformation protocol (CLARITY) was optimized and performed, slightly modified for its application on the cardiac tissue. Indeed, to obtain an efficient reconstruction in 3D of a whole heart, it is essential to prevent the phenomenon of light scattering. The CLARITY methodology allows us to obtain a highly transparent intact heart, but it requires long incubation times when performed passively (about 5 months). With respect to the brain, the cardiac tissue is not suitable for an active clearing, which takes advantage of an electric field. Even at low voltages, the electric field leads to damages and tissue breakages. Here, a passive clearing approach was optimized to obtain a completely cleared heart in about 3 months. After isolating and cannulating the heart through the proximal aorta, the CLARITY methodology was performed as described in section 3 of the protocol. To speed up the procedure, a homemade passive clearing setup was arranged (**Figure 1**), which ended up decreasing the timing of tissue clearing by about 40%. The setup is composed of a container for the clearing solution, a water bath, a peristaltic pump, several chambers containing different sample holders, capsule filters for each chamber, and a tubing system for the recirculation of the solution. The pump extracts and circulates the solution from the container in succession through each of the chambers, where the samples are held for clearing. Before entering the chambers, the solution flows through a capsule filter to trap the lipids flushed away from tissues during the clearing. The optimal temperature for the clearing solution, between $37\text{--}45\ ^\circ\text{C}$, is maintained within the chambers during the recirculation by keeping the solution container in a water bath at $50\ ^\circ\text{C}$. It is advised to change the clearing solution in the container once a week during the procedure. All components used are listed in detail in the **Table of Materials**. The optimized solution presented here allows us to obtain a whole passively cleared mouse heart in a significantly shorter time with respect to the standard passive clearing technique, thus reducing the required experimental time without damaging the organ. The staining approach was also optimized for homogeneous labeling of the cellular membranes and endothelium, using a fluorescent lectin (WGA – Alexa Fluor 633).

The heart cytoarchitecture has been reconstructed by developing a dedicated mesoSPIM that axially sweeps the light-sheet across the sample (<https://mesospim.org>). The custom-made fluorescence light-sheet microscope (**Figure 3**) was able to rapidly acquire images of a mesoscopic FoV (of the order of millimeters) with micrometric resolution. In this way, single cardiomyocytes can be resolved

and mapped into a 3D reconstruction of the entire organ. The microscope illuminates the cleared sample with a light-sheet, dynamically generated by scanning a laser beam at 638 nm using a galvanometric mirror. A sCMOS camera characterizes the detection arm in a 2x magnification scheme which enables it to acquire the entire FoV in a single scan. The fluorescence signal was selected by placing a long-pass filter after the objective. The camera was set to work in rolling shutter mode: at any time, the line of active camera pixels (i.e., exposed to the image) is synchronized with the in-plane shift of the focal band of the light-sheet, performed by an electrically tunable lens. This approach maximized the optical sectioning capability in the whole FoV by only acquiring images in the thinnest part of the focused light-sheet. This solution differs from conventional configurations, where acquisition involves the entire range of focal depth of the light-sheet, preventing peak optical sectioning resolution in large part of the FoV. An integrated sample stage supports cuvettes, thereby optimizing positioning and enabling axial movement of the sample during the imaging process. In this way, tomographic reconstructions are possible by acquiring consecutive internal sections. The images obtained have a mesoscopic FoV and a micrometric resolution, while the acquisition time required for a whole mouse heart is ~ 15 min. The synchronization between the camera rolling shutter and the excitation light beam sweeping the FoV allows acquiring the entire image plane with a high spatial resolution (**Figure 4**). This allows direct reconstruction of the sample in a single tomographic acquisition, without the necessity of sample radial displacement and multi-adjacent-stacks-based imaging. Notably, the microscope allowed the reconstruction of the entire organ of about (10 mm x 6 mm x 6 mm) in a single imaging session, with a near-isotropic voxel size and a sufficient signal-to-background ratio to resolve single cells across the whole organ potentially.

It is noteworthy that the proposed protocol presents some critical steps that must be performed carefully to achieve good results. In particular, the cannulation of the heart through the proximal aorta can be quite difficult, but it is an essential step to wash and fix the organ properly. Judd et al.¹⁷, showed how to perform this step effectively. Moreover, the degassing procedure needed by the CLARITY protocol is quite complex too, but it is essential for tissue preservation; if this step is not performed properly, the tissue could encounter damages and decay during the incubation in clearing solution.

Furthermore, although the presented experimental workflow is suitable for small fluorescent probes, the use of immunohistochemistry does not always provide good efficiency in the staining due to the higher molecular weight of the antibodies. Each immunostaining protocol requires proper optimization, and different approaches have been conceived to improve the antibody penetration, for example, tissue expansion¹⁸ and/or variations in pH and ionic strength¹⁹.

The mesoSPIM setup also presents two main limitations: i) the light-sheet preservation across the sample is strongly dependent on the tissue transparency, and ii) the dimension of the camera sensor limits the FoV. Guaranteeing a perfect refractive index matching inside the entire heart is very challenging, and small variations on the refractive index can produce light scattering, leading to degradation of the image quality. In this respect, a dual-side illumination scheme can be introduced. Two excitation arms can generate two distinct and aligned dynamic light sheets with maximally focused illumination by alternating the illumination from one side to the other of the specimen. Also, the FoV can be improved by using a new generation high-resolution back-illuminated sCMOS with very large sensors in combination with high numerical aperture telecentric lenses with low field distortion. This implementation would allow us to reconstruct bigger organs or expanded tissues maintaining the same optical section capability and thus producing micron-scale 3D images of centimeter-sized cleared samples.

Although the presented protocol still requires a long time for sample preparation and a high level of transparency to obtain a reliable cytoarchitecture reconstruction of the entire organ, the main significance of the approach resides in the improvements of the clearing protocol and the capability to perform mesoscopic reconstruction in a single scan at micrometric resolution. In the future, these advances can be combined with a multi-staining protocol to achieve whole-organ reconstruction integrating different biological structures.

ACKNOWLEDGMENTS:

This project has received funding from the European Union's Horizon 2020 research and innovation program under grant agreement No 95216.

DISCLOSURES:

Nothing to disclosure.

REFERENCES:

1. Cohn, J. N., Ferrari, R., Sharpe, N. Cardiac remodeling-concepts and clinical implications: A consensus paper from an International Forum on Cardiac Remodeling. *Journal of the American College of Cardiology*. **35**, 569–582 (2000).
2. Finocchiaro, G. et al. Arrhythmogenic potential of myocardial disarray in hypertrophic cardiomyopathy: genetic basis, functional consequences and relation to sudden cardiac death. *EP Europace*. **2**, 1–11 (2021).
3. Bishop, M. J. et al. Development of an anatomically detailed MRI-derived rabbit ventricular model and assessment of its impact on simulations of electrophysiological function. *American Journal of Physiology – Heart and Circulatory Physiology*. **298** (2), H699–H718 (2010).
4. Bishop, M. J., Boyle, P. M., Plank, G., Welsh, D. G., Vigmond, E. J. Modelling the role of the coronary vasculature during external field stimulation. *IEEE Transaction on Biomedical Engineering*. **57**, 2335–2345 (2010).
5. Tainaka, K. et al. Whole-body imaging with single-cell resolution by tissue decolorization. *Cell*. **159**, 911–924 (2014).
6. Ueda, H. R. et al. Whole-brain profiling of cells and circuits in mammals by tissue clearing and light-sheet microscopy. *Neuron* **106**, 369–387 (2020).
7. Richardson, D. S., Lichtman, J. W. Clarifying tissue clearing. *Cell*. **162**, 246–257 (2015).
8. Silvestri, L., Costantini, I., Sacconi, L., Pavone, F. S. Clearing of fixed tissue: a review from a microscopist's perspective. *Journal of Biomedical Optics*. **21**, 081205 (2016).
9. Chung, K. et al. Structural and molecular interrogation of intact biological systems. *Nature*. **497**, 332–337 (2013).
10. Park, Y. G. et al. Protection of tissue physicochemical properties using polyfunctional crosslinkers. *Nature Biotechnology*. **37**, 73 (2019).
11. Ding, Y. et al. Light-sheet fluorescence microscopy for the study of the murine heart. *Journal of Visualized Experiments: JoVE*. **139**, 57769 (2018).
12. Olianti, C. et al. 3D imaging and morphometry of the heart capillary system in spontaneously hypertensive rats and normotensive controls. *Scientific Reports*. **10**, 1–9 (2020).
13. Pianca, N. et al. Cardiac sympathetic innervation network shapes the myocardium by locally controlling cardiomyocyte size through the cellular proteolytic machinery. *The Journal of Physiology*. **597**, 3639–3656 (2019).
14. Di Bona, A., Vita, V., Costantini, I., Zaglia, T. Towards a clearer view of sympathetic innervation of cardiac and skeletal muscles. *Progress in Biophysics and Molecular Biology* **154**, 80–93 (2020).

488 15. Voigt, F. F. et al. The mesoSPIM initiative – open-source light-sheet microscopes for imaging
 489 cleared tissue. *Nature Methods*. **16** (11), 1105–1108 (2019).
 490 16. Costantini, I. et al. A versatile clearing agent for multi-modal brain imaging. *Scientific*
 491 *Reports*. **5**, 9808 (2015).
 492 17. Judd, J., Lovas, J., Huang, G. N. Isolation, culture and transduction of adult mouse
 493 cardiomyocytes. *Journal of Visualized Experiments: JoVE*. **114**, 54012 (2016).
 494 18. Yi, F. et al. Microvessel prediction in H&E stained pathology images using fully convolutional
 495 neural networks. *BMC Bioinformatics*. **19** (1), 64 (2018).
 496 19. Susaki, E. A. et al. Versatile whole-organ/body staining and imaging based on electrolyte-gel
 497 properties of biological tissues. *Nature Communications*. **11** (1), 1982 (2020).

498
 499

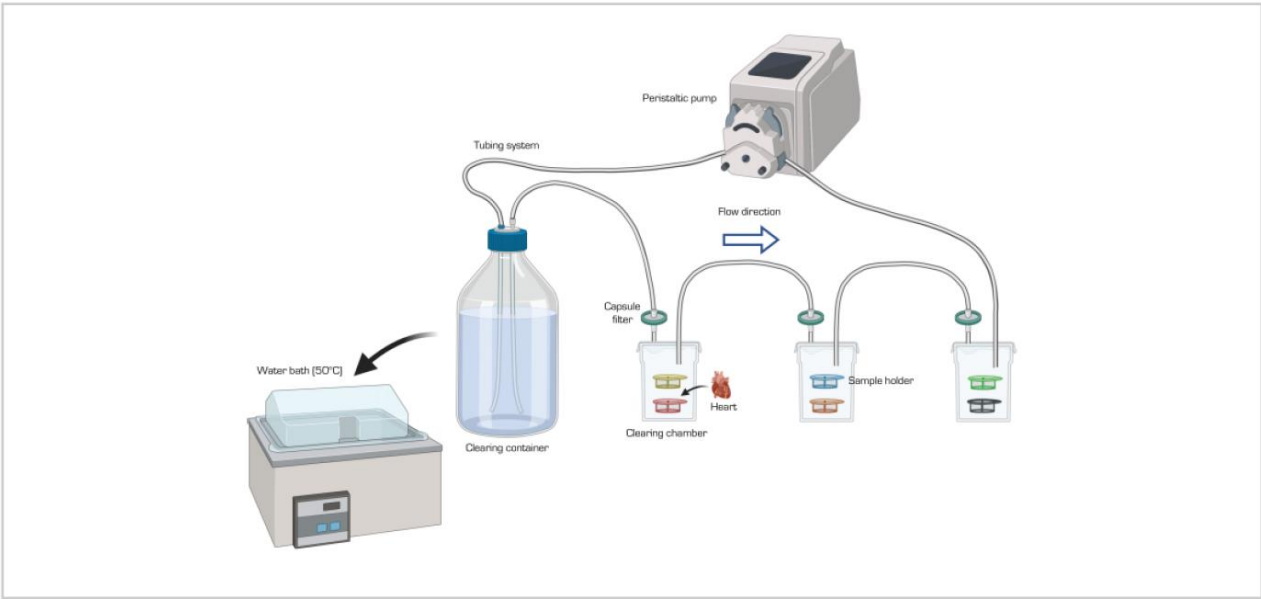


Figure 1

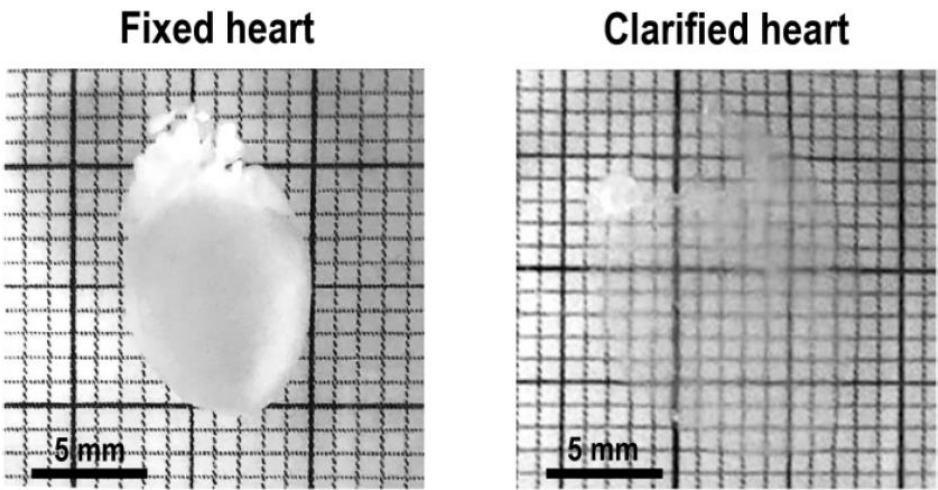


Figure 2

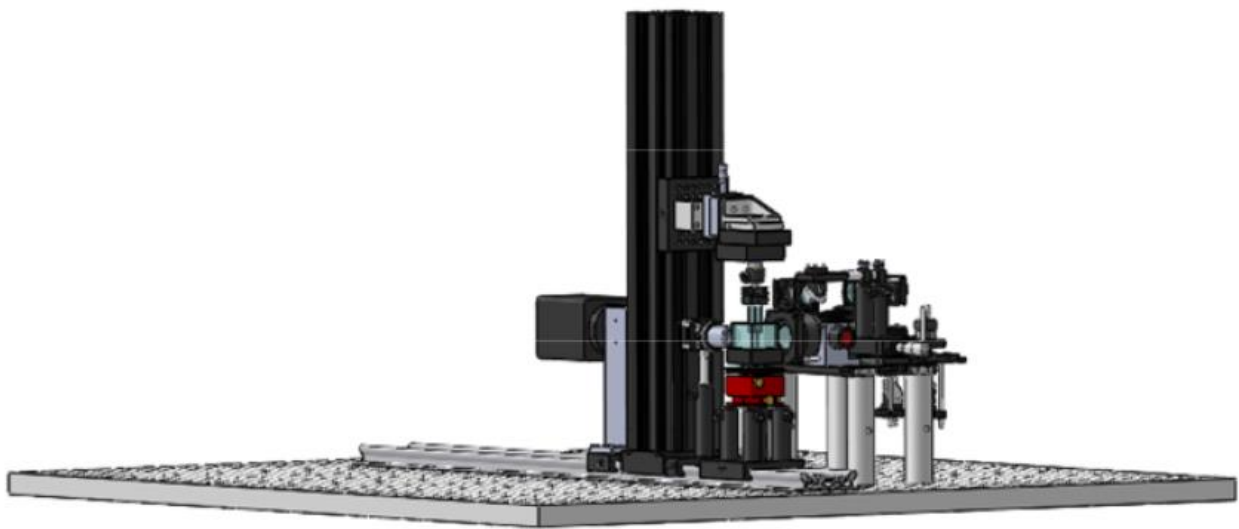


Figure 3

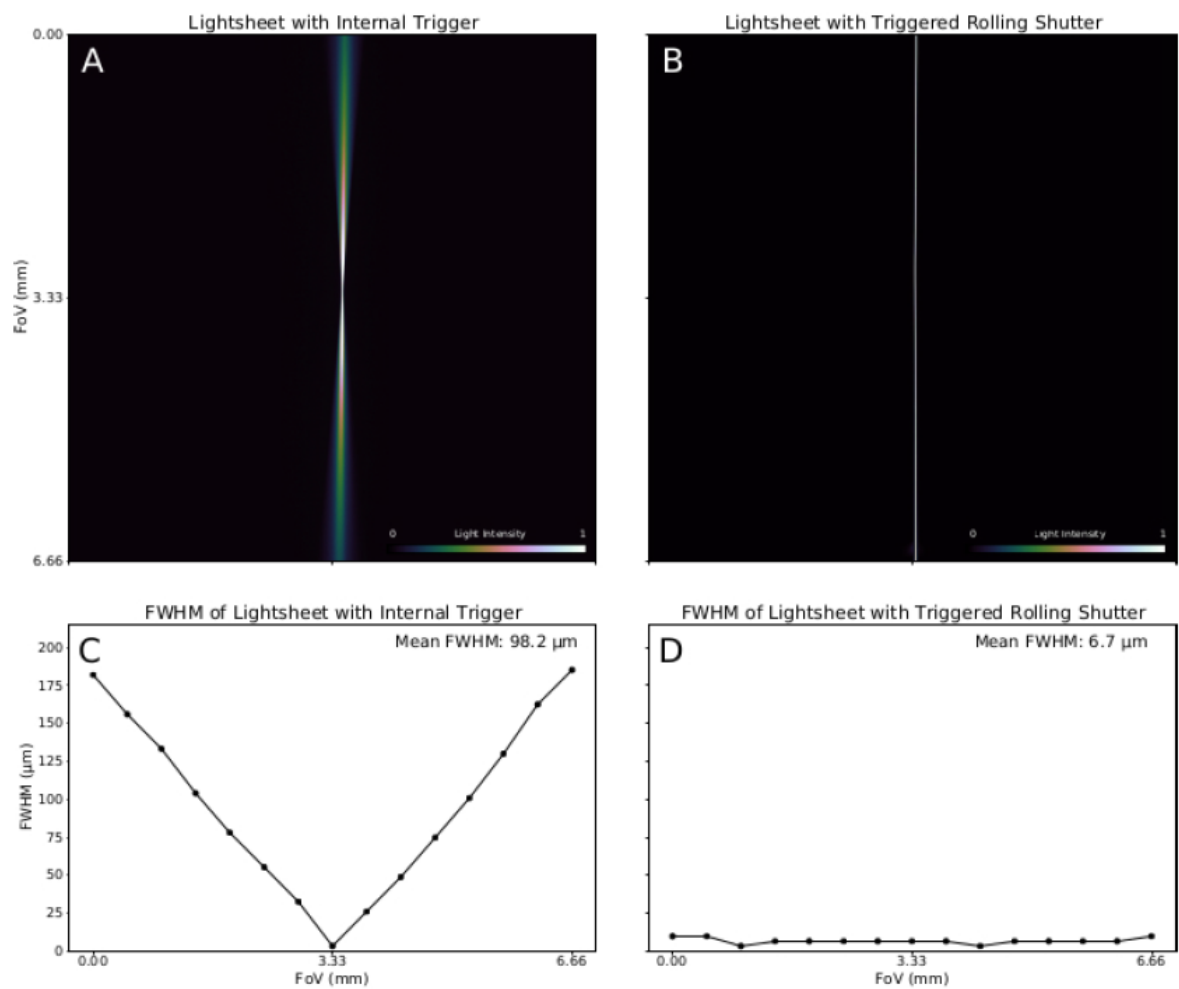


Figure 4

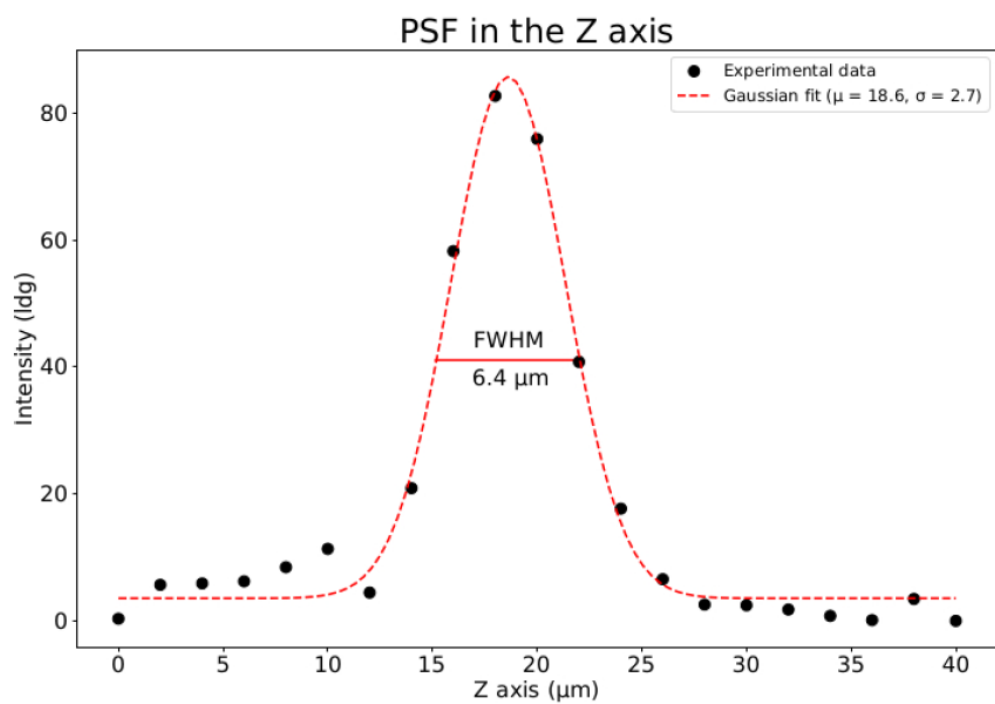


Figure 5

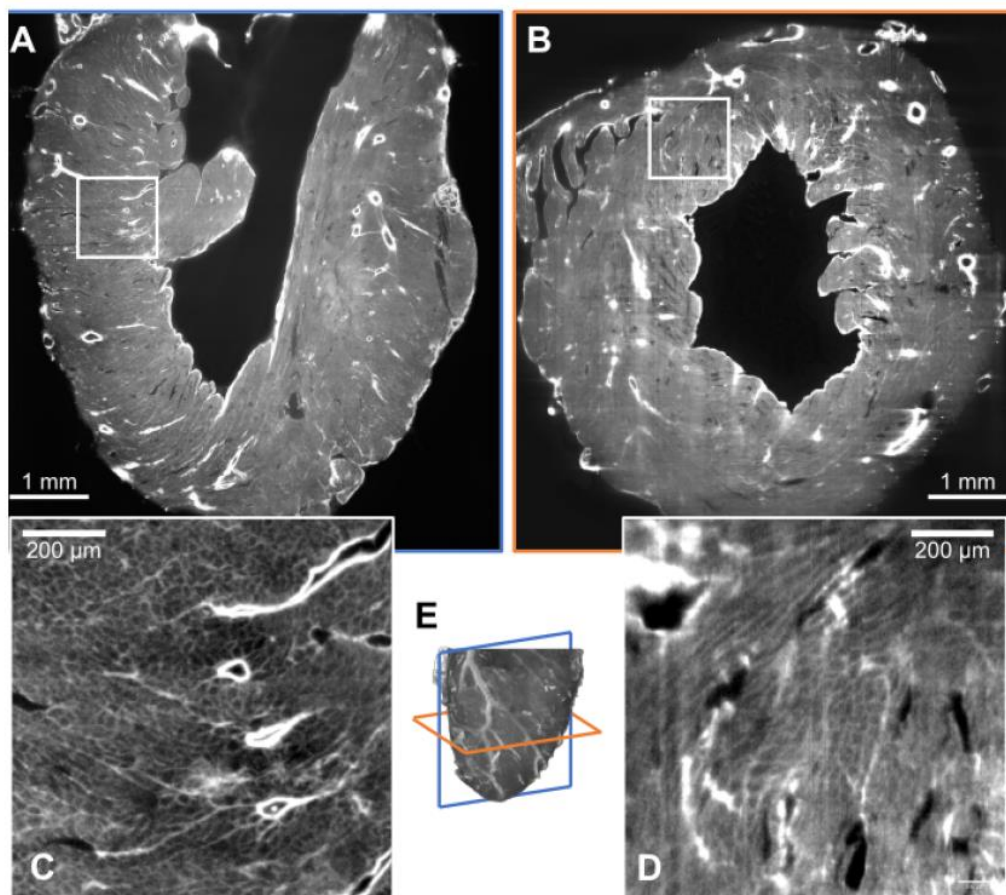


Figure 6